

# A new extraction system for the upgraded AIC-144 cyclotron

Edmund Bakewicz,  
Krzysztof Daniel,  
Henryk Doruch,  
Jacek Sulikowski,  
Ryszard Taraszkiewicz,  
Nikolaj A. Morozov,  
Evgenij V. Samsonov,  
Nikolaj G. Shakun,  
Sergej B. Vorojtsov

**Abstract** This paper is a description of the computer simulation and the first experimental results on an AIC-144 isochronous cyclotron new extraction system. The cyclotron will be able to generate beams of protons, deuterons and  $\alpha$ -particles. One of the principal goals of the upgraded facility is to extract beams of protons and deuterons (proton energy 60 MeV, deuteron energy 30 MeV) for proton radiotherapy and for fast neutron beams. The precession method for particle extraction was chosen as the best one. It is the first time that the proton beam of energy 35 MeV has been extracted from the AIC-144 cyclotron with an efficiency of above 50%. More careful adjustment of the extraction system parameters (better control of the 1st harmonic of the magnetic field and the position of the deflectors) will permit an increase in the extraction efficiency to the design value of 70%.

**Key words** cyclotron • extraction system • deflector • magnetic channel • proton beam

## Introduction

The AIC-144 isochronous cyclotron [6] designed and constructed at the Institute of Nuclear Physics in Kraków will be able to generate beams of protons, deuterons and  $\alpha$ -particles. One of the principal goals of the new facility is to extract beams of protons and, possibly, deuterons (proton energy 60 MeV, deuteron energy 30 MeV) for proton radiotherapy and for horizontal and vertical fast neutron beams.

It was extremely important to select the best and most efficient extraction system for the cyclotron [1-4]. The problem of the effective beam extraction was found difficult, considering constraints of the existing cyclotron. The precession method for extraction was agreed on as the right one. One of the most important issues was the control of the 1st harmonic of the magnetic field distortion due to the deflection system in the area of the internal circulating beam. It was important to measure the effect of such a magnetic field distortion and to introduce the measured data into the computer codes for beam dynamics calculations. The requirement to have realistic fringe field maps, including the field inside the magnetic channels, stimulated the necessary measurements of the field. The means to correct the possible field distortion due to removal of the ferromagnetic material from the valley between sectors for installation of new harmonic coils were foreseen. Optimization of various parameters of the proposed extraction system, e.g. positions, field, gradients, etc. were included into the upgrading programme. It was useful to modify the field in order to shift the position of the coupling resonance to limit the axial blow-up of the beam by

E. Bakewicz, K. Daniel, H. Doruch, J. Sulikowski,  
R. Taraszkiewicz<sup>✉</sup>  
Henryk Niewodniczanski Institute of Nuclear Physics,  
Cyclotron Section,  
152 Radzikowskiego Str., 31-342 Kraków, Poland,  
Tel.: +4812/ 6370222 ext. 365, Fax: +4812/ 6375441,  
e-mail: tarasz@alf.ifj.edu.pl

N. A. Morozov, E. V. Samsonov, N. G. Shakun,  
S. B. Vorojtsov  
Joint Institute for Nuclear Research,  
Laboratory of Nuclear Problems,  
6 Joliot Curie Str., RU-14198 Dubna, Russia

Received: 25 September 2000, Accepted: 12 March 2001

including appropriate valley shims and other available means. The central region structure was investigated in detail to obtain the necessary beam quality in the pre-extraction region. The non-linear effects inside extraction elements were taken into account to prevent deterioration of the beam emittance. Matching of the extraction beam and the downstream beam transport system acceptance was performed. Electrostatic and magnetic channels were designed with special care.

Beam extraction experiments were carried out for the proton beam of final energy 35 MeV. This regime had the following parameters: the main coil current 169.2 A, the optimal radio frequency 20.0 MHz, the isochronous magnetic field at the machine center 13.250 kG, the accelerating dee voltage 45 kV. Intensive simulation of particle motion and necessary alignments of the extraction system structure elements accompanied beam measurements.

The layout of the cyclotron chamber with the new extraction system is given in Fig. 1.

### Calculation of particle dynamics

#### Radial gain enhancement

Beam dynamics simulation was performed with a set of programs described in [5]. A bunch of 100 particles randomly distributed inside 5-dimensional phase space volume ( $r, r', z, z', \text{HF-phase}$ ) at an energy of 31 MeV ( $r \approx 60 \text{ cm}$ ) was chosen as the initial condition for computation of particle dynamics. Initial amplitudes of radial and axial oscillations were 5 and 3 mm, respectively. The phase width of the bunch was  $40^\circ \text{HF}$  and the position of central particle  $30^\circ \text{HF}$ . This special negative shift of the central particle phase is created in the cyclotron by the appropriate form of an average magnetic field in order to compensate a positive phase shift of about  $50^\circ \text{HF}$  that arises in a fringe field of the machine. The number of acceleration turns that a particle has to make to appear at the entrance of the extraction sys-

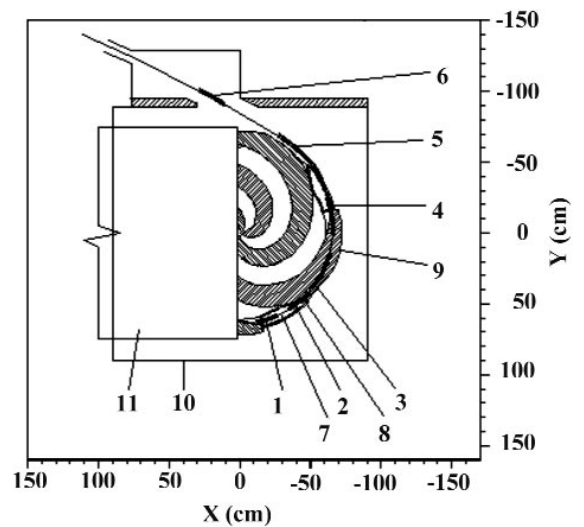


Fig. 1. Cyclotron chamber with the extraction system. 1,2,3 – electrostatic deflector sections ESD-1,2,3; 4,5,6 – magnetic channel sections MC-1,2,3; 7 – valley shim; 8 – harmonic coil; 9 – spiral shim; 10 – vacuum chamber; 11 – dee.

tem varied from 60 to 70 depending on its initial conditions.

The radial distributions of the magnetic field parameters at the edge region of the cyclotron are shown in Fig. 2. The amplitude of the 1st harmonic of the magnetic field is close to 2 G and its phase varies between  $-40^\circ$  and  $0^\circ$ , while the entrance of the extraction system is located at the azimuth  $120^\circ$ . These parameters of the 1st harmonic were obtained with the field of B1 coils located at radii  $55 \pm 65 \text{ cm}$  and with allowance for measurements of magnetic field imperfections at the edge region of the cyclotron. The 1st harmonic phase was specially optimized to minimize the particle losses on external side of the electrostatic deflector septum. As a result of computations, losses of this type do not exceed 3% of the internal beam.

Fig. 3 shows the particle betatron frequencies in the cyclotron regime considered. Particles cross resonances of three types:  $Q_r=1$ ,  $Q_z=0.5$  and  $2Q_z=Q_r$ . The most danger-

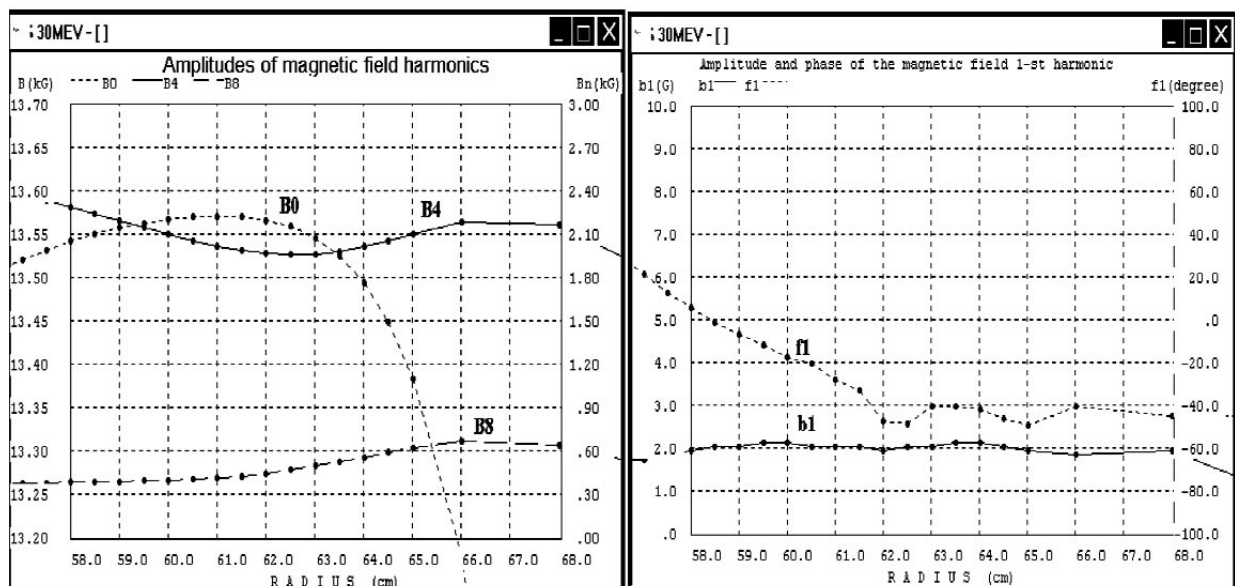


Fig. 2. Magnetic field parameters at the edge region of the cyclotron AIC-144. Left-side plots show the average field  $B_0$  and the amplitudes of the 4th ( $B_4$ ) and 8th ( $B_8$ ) harmonics. Right-side plots show the amplitude of the 1st ( $b_1$ ) harmonic and its phase ( $f_1$ ).

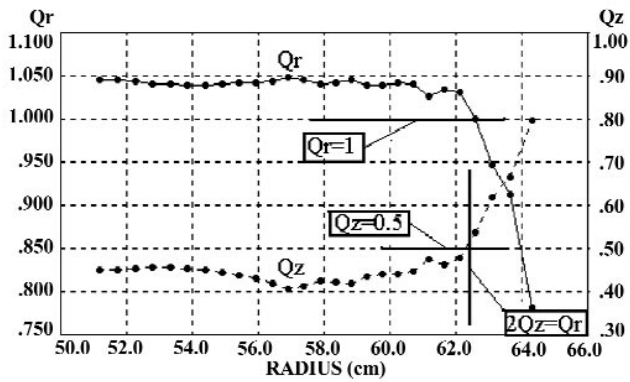


Fig. 3. Particle betatron frequencies at the edge region of the cyclotron.

ous resonance is the third one, excited by nonlinearity of the average magnetic field and causing an increase in the axial beam size. In order to limit the influence of this resonance one should use small amplitudes of the betatron oscillations (3÷5 mm) and the 1st harmonic of the magnetic field has to be restricted with in the value (2÷3 G) at the edge region of the cyclotron.

Fig. 4 represents the results of particle dynamics simulation on a radial phase plane. The positions of 100 particles are indicated stroboscopically at the azimuth of the extraction system entrance (120°) one time after each turn until each particle appears in the aperture of the first element of the extraction system. One sees enhancement of the radial gain per turn up to 7 mm at this moment. Computations show that the resonance  $2Q_z = Q_r$  leads to the axial beam size increase approximately by 60%. Radial and axial emittances of the beam on the entrance of extraction system were equal to  $\sim 15\pi$  mm·mrad and  $\sim 10\pi$  mm·mrad, respectively. Energy of the beam was  $35.1 \pm 0.1$  MeV. Particle losses were distributed in the following way: 7% particles were lost at the front edge of the septum (thickness 0.5 mm) and 3% on the outer side of the septum. Thus, up to 90% of the internal beam could be extracted from the cyclotron. Of course, some additional losses inside the extraction system decrease this value.

Beam deflection, extraction system element requirements

The extraction system of the AIC-144 cyclotron consists of 6 elements located inside the vacuum chamber (see Fig. 1): 3 electrostatic deflectors and 3 magnetic channels. They have the following denotations and azimuth positions: ESD-1 – (98÷117)°, ESD-2 – (120÷140)°, ESD-3 – (140÷177)°, MC-1 – (183÷205)°, MC-2 – (215÷250)°, MC-3

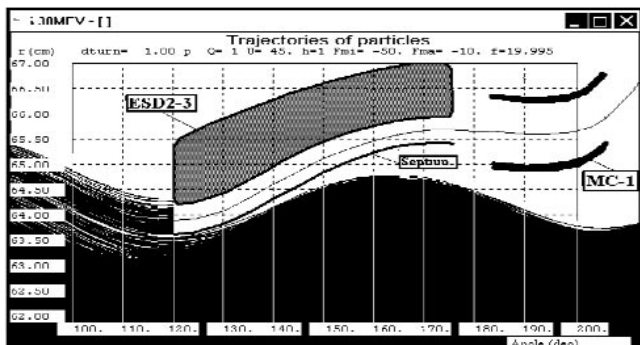


Fig. 5. Particle trajectories at the region of ESD-2, 3 and MC-1.

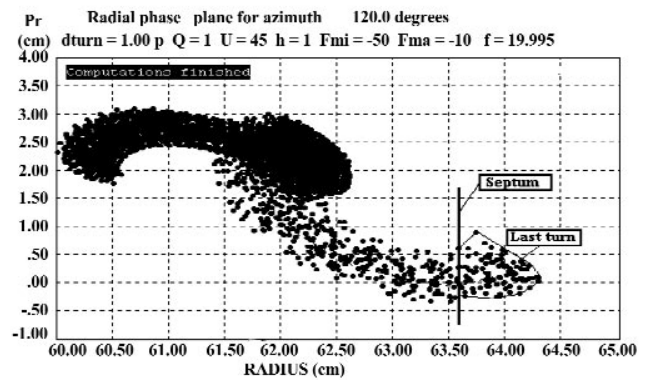


Fig. 4. Results of particle dynamics computation on the radial phase plane at the azimuth of the extraction system entrance.

– (273÷283)°. The 2nd and 3rd electrostatic deflectors are mounted on the same case and are powered by one high-voltage unit. This set of elements is proposed to be used for extraction of 60 MeV protons. For extraction of 35 MeV protons the 1st electrostatic deflector can be removed from the vacuum chamber. The remaining elements are able to extract the beam to the matching point. The matching point, where beams of various energies and type of particles should be extracted to, has the coordinates  $\phi=308^\circ$ ,  $r=153$  cm, and is just in front of the first element of the transport line.

In Table 1 the required parameters of the extraction system that correspond to proton energy of 35.1 MeV are presented. The focusing gradients of the electric and magnetic fields are used inside ESD-3, MC-2 and MC-3 in order to compensate the defocusing effect (in horizontal plane) of the fringe magnetic field. The elements ESD-2 and MC-1 have a uniform field inside their working apertures.

Fig. 5 shows the boundary of the circulating beam together with the trajectories of particles just before the entrance of ESD-2 and the central trajectory of the extracted beam. One can see that ESD-2, 3 permit the extracted beam to be deflected by about 10 mm from the boundary of circulating beam.

The beam envelopes along the central line of the deflection system are presented in Fig. 6. Computations show that particle losses inside ESD-2, 3 do not exceed 20%, if the deflector aperture is 7 mm. The voltage of 40 kV across the ESD-2, 3 electrodes corresponds to this aperture of the deflectors. No particle losses were observed inside the magnetic channels. Hence, taking into account 10% losses of

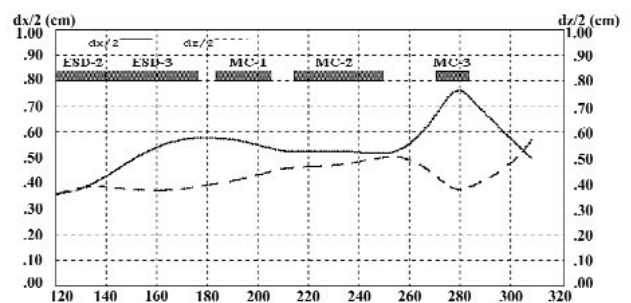


Fig. 6. Beam envelopes along the central line of the deflection system.

**Table 1.** Parameters of the extraction system for proton energy of 35.1 MeV.

Element	$\phi_1$ ( $^\circ$ )	$\phi_2$ ( $^\circ$ )	$r_1$ (cm)	$r_2$ (cm)	$\Delta B$ (kG)	$\epsilon$ (kV/cm)	$dB/dx$ (kG/cm)	$d\epsilon/dx$ (kV/cm <sup>2</sup> )
ESD-2	120	140	63.85	64.60	–	58.3	–	0.0
ESD-3	140	177	64.60	65.69	–	48.9	–	–20.4
MC-1	183	205	65.66	65.99	–1.582	–	0.0	–
MC-2	215	250	66.83	75.17	–2.153	–	0.8	–
MC-3	273	283	88.37	98.33	0.0	–	1.0	–

particles before deflection, one should estimate the efficiency of extraction as being equal to 70%.

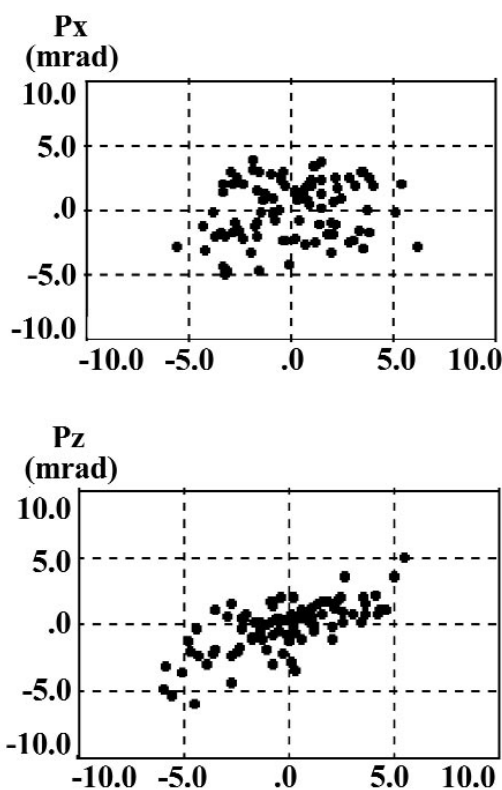
The phase portraits of the beam at the matching point are shown in Fig. 7 for the horizontal and vertical planes. The spot beam dimensions are  $\sim 10 \times 10$  mm<sup>2</sup>.

### Structural elements

#### Electrostatic deflectors

The electrostatic sections are shown in Figs. 8 and 9. The septum parts of the sections are water-cooled. The entrance part of the septum (thickness 0.1 mm) is made of tungsten. C-shaped skeleton (stainless steel) of the deflectors allows a high accuracy of the required septum curvature at thermal loading on the septum due to beam losses up to several hundreds watts.

The high-voltage electrode (titanium) is not cooled by water, its entrance part is protected against beam particles by a special C-shaped diaphragm. The deflectors have a remote drive for radial moving and changing of the inclination angle in relation to the beam trajectory.

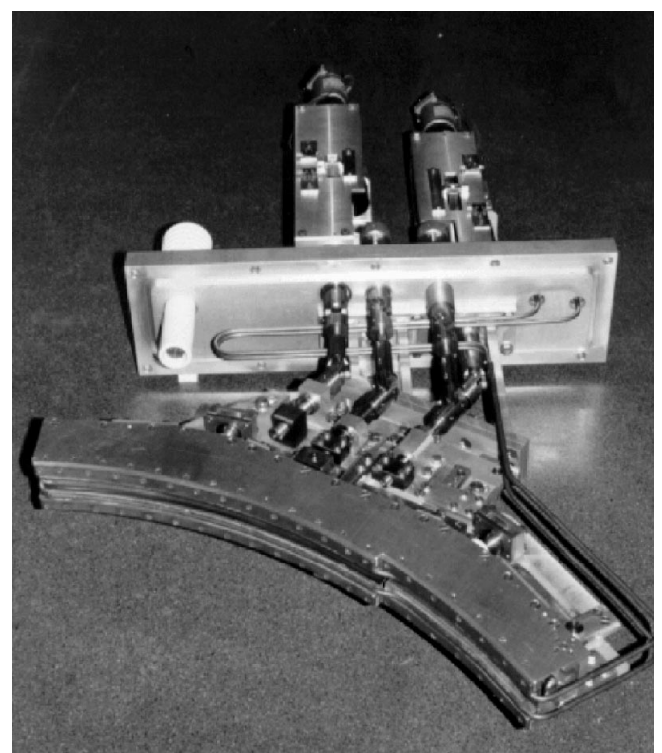
**Fig. 7.** Phase portraits of the beam at the matching point.

The gap between the septum and the high-voltage electrode is adjusted within the limits of 4–15 mm without opening of the cyclotron chamber. Another adjustment of the gap can provide a varying gap within the limits of 10 mm along the beam trajectory. Preliminary training of the sections was carried out by high voltage within 12 hours. For extraction of protons with energy 35 MeV, a gap of 5.5 mm at the entrance and 6.5 mm at the exit of section was made between the septum and the high-voltage electrode of the section ESD-2, 3. The working voltage was 45 kV (the calculation voltage was 40 kV).

#### Magnetic channels

The system of magnetic channels consists of two passive channels MC-1, 2 (Figs. 10 and 11) and an electromagnetic channel MC-3 (Fig. 12). In the channel MC-1, the magnetic field is homogeneously decreased by  $\sim 0.18$  T by means of steel plates with the cross dimensions  $2.5 \times 30$  mm<sup>2</sup>. In the channel MC-2, the magnetic field is decreased by  $0.18 \pm 0.22$  T and the radial-focussing gradient 8 T/m is introduced by means of steel plates with the cross dimensions  $(2.5-5) \times 50$  mm<sup>2</sup>.

Additional steel plates in the channels MC-1, 2 are placed in on aluminum C-shaped case to shim the magnetic field distortion caused by the channel in the region of the accelerated beam (the average magnetic field distortion and the first harmonic are shimmed down to the several gauss).

**Fig. 8.** Electrostatic deflector ESD-2-3, top view.

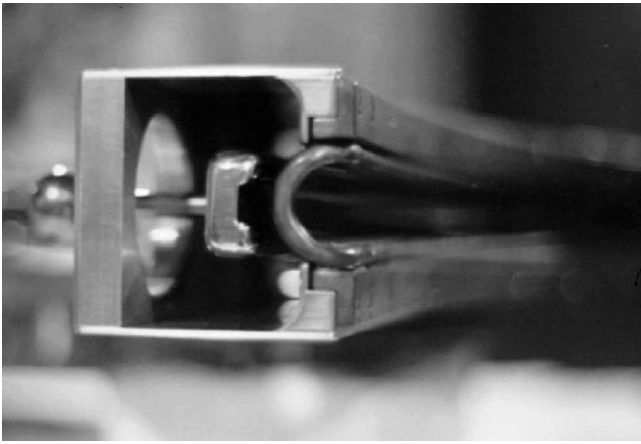


Fig. 9. Electrostatic deflector ESD-3, rear side.

The magnetic channel MC-3 is a small ( $100 \times 100 \times 150 \text{ mm}^3$ ) electromagnetic quadrupole lens with an aperture of 30 mm in diameter, which can focus a beam in a radial direction with a gradient up to 20 T/m at a maximum level of its coil power dissipation of 1.9 kW. In region of the accelerated beam the channel MC-3 creates the field perturbation not exceeding several gauss (for average field and first harmonic). All magnetic channels have remote adjustment of their radial position in the chamber of the cyclotron. The channel MC-3 has also additional adjustment of its angular position.

#### Coils for the 1st harmonic shaping

The amplitude and the phase of the first harmonic of the magnetic field near the radius 60 cm are the parameters determining the characteristics of the beam turn separation enhancement in the electrostatic deflector mouth. The required characteristics of the first harmonic of the magnetic field ( $B_1 = 2 \text{ G}$ ,  $\varphi_1 = 0$  – the phase is directed along the dee axis) were shaped by means of new cyclotron harmonic coils [8]. The results of correcting the first harmonic amplitude by means of the coils are shown in Fig. 13.

### Experimental results

#### Beam centering and amplitudes of betatron oscillations

In order to meet the requirements to the amplitudes of betatron oscillations ( $a_r \leq 5 \text{ mm}$ ,  $a_z \leq 3 \text{ mm}$ ) some modifica-

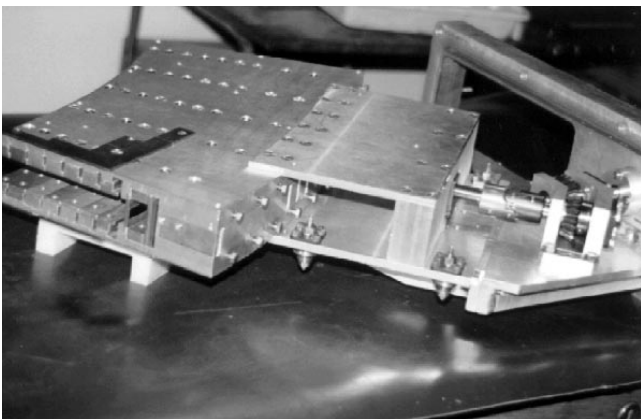


Fig. 11. Magnetic channel MC-2, entrance side.

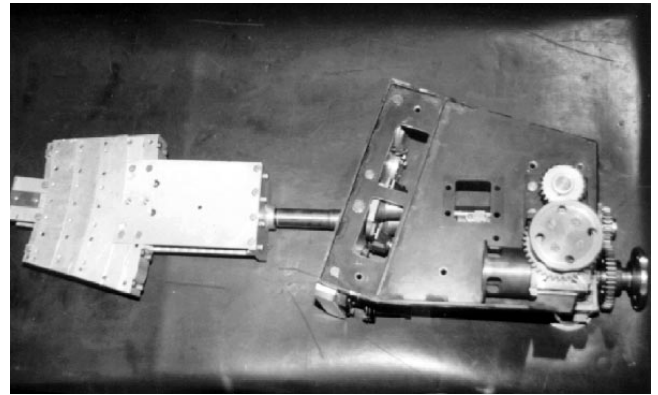


Fig. 10. Magnetic channel MC-1, top view.

tions were done to the central cyclotron region geometry. Two diaphragms with an angular distance of  $180^\circ$  between them were installed on the 1st and 2nd turns of the beam. The dimensions of the slits intended for the beam pass were  $(\Delta r, \Delta z) = (1 \times 10) \text{ mm}^2$  and  $(2 \times 10) \text{ mm}^2$ . Fig. 14 shows current distribution at the center of the cyclotron obtained by means of the differential probe with lamellas of radial thickness 1 mm. This current measurements and their comparison with the results of computations demonstrate that the beam is centered with an accuracy of  $1 \div 2 \text{ mm}$  and has an incoherent radial amplitude  $\leq 2.5 \text{ mm}$ .

The 1st harmonic with the amplitude  $\sim 5 \text{ G}$ , which exists in the main acceleration region of the cyclotron, leads to beam decentering up to 7 mm near the radius 50 cm. But a smooth decrease in the 1st harmonic to 2 G, which is ensured by special B1 coils at the radius 60 cm, causes a corresponding decrease down to 2 mm of beam decentering. This effect of the 1st harmonic (which is due to a quite large number of beam turns ( $\sim 150$ ) between the radii 50 and 60 cm) was computed and confirmed by the beam shadow measurements at the cyclotron. These measurements also proved that incoherent radial oscillations did not exceed 2 mm. Thus, the sum of radial oscillations had the amplitude not more than 4 mm. Axial amplitudes were decreasing during acceleration from 5 mm to 3 mm because of betatron axial frequency increasing from 0.15 ( $r = 10 \text{ cm}$ ) to 0.4 ( $r = 60 \text{ cm}$ ).

Note, that there were practically no particle losses during the acceleration process in the radial range  $10 \div 50 \text{ cm}$  (see Fig. 15). The Figure also shows that the beam intensity decreases in the radial region  $50 \div 60 \text{ cm}$ . The radial beam density dilution near the radius of 61 cm could be explained

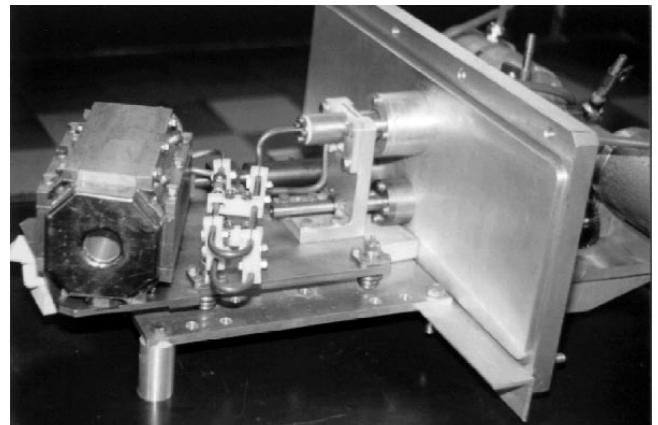


Fig. 12. Magnetic channel MC-3, entrance side.

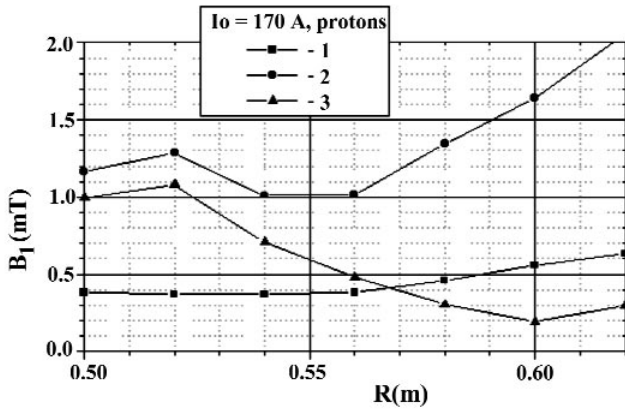


Fig. 13. First harmonic amplitude of the magnetic field. 1 – magnetic channels are not mounted, 2 – magnetic channels are mounted, 3 – effect of magnetic channels is corrected by harmonic coil contributions.

by the effect of the extraction system. More detailed description of the beam behavior in this particular region is given in the next section.

Measurement of radial gain enhancement

In order to measure the radial gain enhancement a special 5-lamella probe was used. This probe was installed at the azimuth 118°, i.e. 2° upstream the entrance of the ESD-2, the first element of the extraction system for the beam energy considered. Radial thickness of the 1st lamella was 0.5 mm, the thickness of others was 2 mm. The vertical dimension of the lamellas was 20 mm. Fig. 16 shows the results of measuring current distributions between the lamellas. An increase in radial gain just before the extraction is clearly seen. The absolute current value was somewhat higher in this experiment as compared with the intensity value in the beam centering measurements, Fig. 14.

Extraction efficiency

The following procedure has been applied to make the extraction system operational:

- measurement of the radial gain enhancement without the extraction system inside the vacuum chamber;
- the same but with ESD-2, 3 at their working position in order to measure probable particle losses on the outer side of the septum;

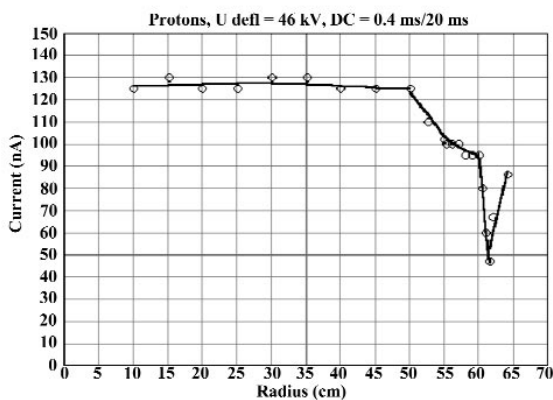


Fig. 15. Accelerated beam current performance; circles – measurements; solid line – piecewise polynomial fit.

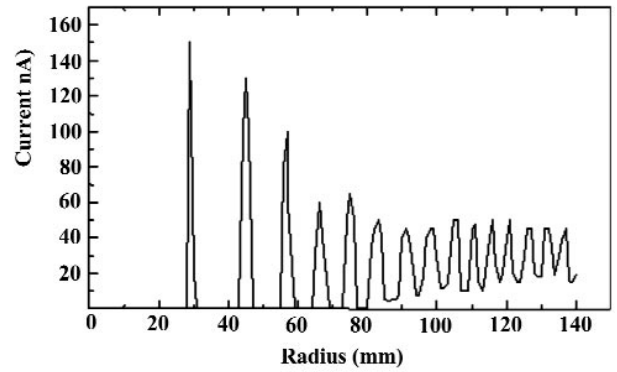


Fig. 14. Current distribution at the center of the cyclotron after installation of two diaphragms.

- beam passage through ESD-2, 3, measurement of the particle losses inside them;
- step by step installation of the magnetic channels MC-1, 2, 3, the corresponding tuning of the radial gain enhancement, and measurement of the beam transport efficiency at each step.

We observed a very high efficiency (~85%) of the beam deflection at the exit of ESD-3 when no magnetic channels were installed inside the vacuum chamber. Installation of the magnetic channels requires additional efforts to compensate the 1st harmonic in order to improve the process of radial gain enhancement. This procedure was not very long. As a rule, 1+2 h were enough to obtain the extracted beam with efficiency above 50%. No particle losses were detected inside the magnetic channels. It is interesting to note that in the previous experiments (before the upgrading program was fulfilled) on 18.6 MeV deuteron beam extraction from the machine by methods other, than the at given above, the extraction efficiency was not greater than 7% [7]. We believe that longer and more accurate adjustment of the extraction system parameters (mainly careful control of the 1st harmonic of the magnetic field and the position of ESD-2, 3) will permit us to increase the extraction efficiency up to the design value of 70%.

To visualize the extracted beam in the window of the vacuum chamber we used a luminescent target and a television

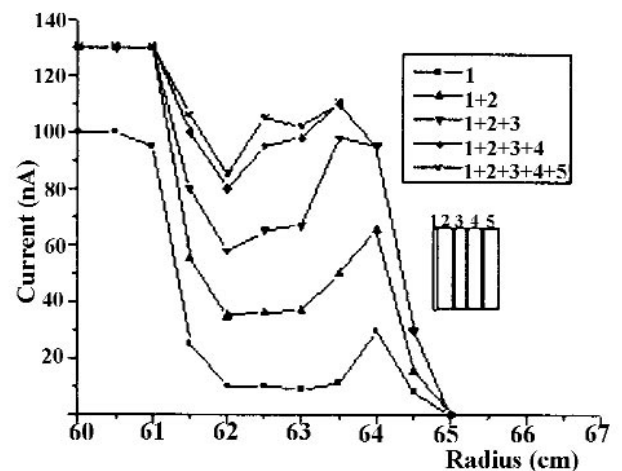


Fig. 16. Measurement of current distribution between probe lamellas.

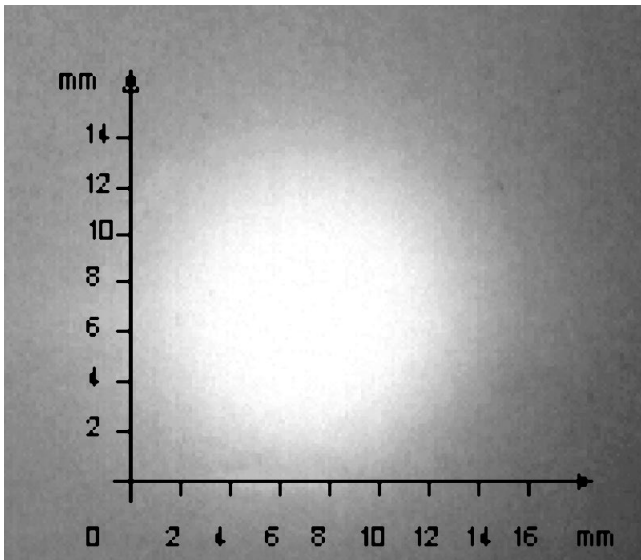


Fig. 17. Television image of the beam spot in the window of the vacuum chamber.

camera. Fig. 17 shows the beam spot on this target. The position and the size of the beam closely agree with the computational results.

### Conclusions

It is the first time that the proton beam of energy 35 MeV has been extracted from the AIC-144 cyclotron with efficiency above 50%.

More careful adjustment of the extraction system parameters (better control of the 1st harmonic of the magnetic field and the position of ESD-2, 3 as major factors) will permit an increase in the extraction efficiency to the design value of 70%.

**Acknowledgments** The authors would like to express their special gratitude to Prof. A. Budzanowski, director of the Institute of Nuclear Physics in Kraków, for his continuing interest in and support of this work. The authors are very much indebted to all members of the cyclotron section staff and other technical workers of the INP (Kraków). Without their great efforts it would be impossible to fulfil the given beam experiments at the AIC-144 cyclotron.

The work was supported by the NAEA (National Atomic Energy Agency of Poland).

### References

1. Borisov ON, Morozov NA, Samsonov EV *et al.* (1996) Feasibility study of the beam extraction from the AIC-144 Cyclotron. Report JINR E9-96-492. Dubna, Russia
2. Borisov ON, Morozov NA, Samsonov EV *et al.* (1997) Feasibility study of the beam extraction from the AIC-144 Cyclotron European Cyclotron Progress Meeting (1997). In: ECPM XXXI, 18–20 September 1996, Gröningen. Abstracts: 24–26
3. Borisov ON, Morozov NA, Samsonov EV *et al.* (1998) New beam extraction system for the AIC-144 cyclotron. JINR, E9-98-130, Dubna
4. Borisov ON, Morozov NA, Samsonov EV *et al.* (1998) New beam extraction system for the AIC-144 cyclotron. In: Proceedings of the 15th Int Conf on Cyclotrons and their Applications, 14–19 June 1998, Caen, France. Institute of Physics Publishing, Bristol and Philadelphia, pp 528–530
5. Samsonov EV (1996) Methods used in the calculation of the ion beam injection and acceleration of the VINCY cyclotron. In: Proceedings of the Workshop on the Magnetic Field and Ion Beam Dynamics of the VINCY Cyclotron, March 11–15 1996. JINR, Dubna
6. Schwabe A, Starzewski, Semkowicz A (1978) Automatic isochronous cyclotron AIC-144. In: Proceedings of the International Seminar on Isochronous Cyclotron Technique, 13–18 November 1996, Kraków, Poland. Report IFJ N 1069/PL, pp 197–215
7. Schwabe JA (1997) AIC-144 – Automatic isochronous cyclotron. Main parameters, status. *Nukleonika* 42;3:727–770
8. Vorojtsov SB, Morozov NA, Bakewicz E *et al.* (2000) Harmonic coil application for shaping of the magnetic field of isochronous cyclotron AIC-144. Communications of the JINR P9-2000-39, Dubna (in Russian)